Semi-Automated Method to Extract Urban Areas from Barren Land/ Bare Soil, Case Study: Idku, Nile Delta Coast, Egypt

Hanady H. Khalil* and Mahmoud Hassaan

Institute of Graduate Studies and Research, Alexandria University, Alexandria, Egypt

Received: 8 July 2019, Revised: 26 November 2019, Accepted: 3 December 2019

Abstract

Optical remote sensing offers a time and cost-effective manner to monitor urban-form expansion over time. The availability of recent and historical remote sensing data together with the wide coverage of these data make remote sensing application further favorable for the purpose. However, urban areas surrounded by barren land/ bare soil tend to be overestimated due to the similar spectral behavior of both urban areas and their surroundings. This paper aims to develop a methodology that overcomes the interference between urban areas and barren land/ bare soil and thus enhances the urban areas' extraction in a semi-automated manner. For this purpose, SAVI, NDBI and MNDWI indices, PCA and thermal band were employed to extract urban areas from their surroundings in two Landsat images for the years 1998 and 2016. The developed methodology was applied to extract urban form of Idku Town, one of the coastal urban centers of the Nile Delta, with an overall accuracy of 96.48% and 93.39% for the images of 1998 and 2016, respectively. The results have revealed that the urban form of Idku Town was tripled over the last two decades with an annual growth rate of about 12%.

Keywords: urban-form, Barren land, bare soil, remote sensing
DOI 10.14456/cast.1477.9

1. Introduction

Unplanned rapid urban expansion and its associated change in land use/land cover pattern place a heavy burden on environmental resources and have serious environmental consequences, for example, urban expansion usually alters local climate (usually referred to as microclimate), creates heat island effect and accordingly increases energy demand and costs of new infrastructure [1-10]. Therefore, regular and continued monitoring of urban-form expansion is required [11-13] to predict urban growth, to understand its dynamics, to define energy needs and to learn about changes in microclimate. Monitoring urban-form expansion starts with delineating urban areas out of their surroundings in a fast and cost-effective manner. Delineating urban areas is a basic step in many researches especially those related to heat islands, microclimate and climate change [7].

*Corresponding author: Tel.: +203 424-9290 Fax: +203 424-9290
E-mail: hanady.h.khalil@gmail.com

Optical remote sensing provides a reliable mapping of urban areas through many techniques including automated and semi-automated techniques [14, 15]. Due to the dynamic nature of urban areas expansion, applying conventional approaches in monitoring urban expansion such as aerial photography, surveys and/or cartography is questionable. This is because they are usually time, money and effort consuming in addition to their unavailability over long time span in many cases [11, 12]. Instead, remotely-sensed data provides a powerful source of knowledge in monitoring rapid urban expansion over long periods of time. For this reason, remote sensing imagery has been used repeatedly in monitoring and assessing urban expansion and consequent changes in land use/land cover through discriminating urban land from non-urban land in a fast and cost-effective manner [16, 17].

Delineating urban areas from remote sensing imagery depends mainly on their spectral behavior that, in turn, determined by their physical characteristics and chemical composition. Thus, it is important to understand the physical characteristics of urban areas that govern their spectral behavior in order to distinguish them as a first step towards identifying their spatial extent and quantifying their development through remotely sensed data [12].

There are two distinguished approaches to extract urban areas from remote sensing data which are classification techniques [18, 19] and spectral indices [20, 21]. Both of these approaches depend on the spectral behavior of different land covers, but they work differently. Both have their advantages and limitations but indices have a virtue over classification in terms of time needed to generate them [22]. Classification techniques are laborious, time-consuming and expert-dependent techniques. Moreover, there is a problem in differentiating urban areas and barren land/ bare soil under classification techniques as both have similar response at some places leading to overestimation of urban lands [7]. Spectral indices are favorable and frequently employed to enhance a desired land cover in order to detect its changes over time. The powerful point about indices is that they are selective, fast and easy to implement and totally automated. Indices use the spectral response of a certain land cover to enhance and manifest it on the expense of other land covers. Normal Difference Water Index (NDWI) and Modified Normal Difference Water Index (MNDWI) [17, 23] are examples of these selective indices as they make water bodies much more remarkable on the expense of vegetation and land. The same goes for other indices such as Normal Difference Vegetation Index (NDVI) [24], Soil-Adjusted Vegetation Index (SAVI) [25] and Normal Difference Built-up Index (NDBI) [17, 20, 21]. Each of these indices focus on the desired land cover and make it easier to be extracted and make it possible to identify different classes related to this particular land cover in a relatively higher accuracy.

Many indices, such as NDBI, have been developed to enhance built-up areas in order to extract them in an automated manner. Although NDBI enhances the urban areas in a notable manner, it has its limitations when the scene contains barren land/ bare soil, dry vegetation and/or water of high-suspended matter. Urban areas tend to mix up with barren land/ bare soil leading to overestimation of built-up areas [3, 7, 9, 14, 15]. Likewise, some vegetation and water surfaces under certain conditions may give positive value in the NDBI and hence misclassified as urban areas [17].

Despite the limitations of NDBI, it still works well to separate built-up and barren land from other land covers (water and vegetation). Yet, mapping urban areas out of barren lands through such an index is challenging due to the similarity in spectral behavior of both [3, 7, 9, 14, 15] especially in Mediterranean cities as they have very low vegetation cover in rural areas, scarce rains and land covers lacking moisture [7]. Therefore, there is always a need for improved techniques considering the similarity of urban areas spectral response with their adjoining barren land/ bare soil. Several studies suggested that NDBI should not be used alone but in a combination with NDVI and NDWI [15, 17, 26] to enhance its performance.

The purpose of this paper is to develop a systematic, semi-automated methodology to extract urban areas out of barren land/ bare soil areas using remote sensing data and to detect the

long-term change in urban-form. The developed methodology is applied to one of the Nile Delta coastal urban areas; Idku Town, Egypt.

2. Materials and Methods

2.1 Study area

Idku Town is one of the Egyptian urban centers located in the coastal zone of the Nile Delta. As many of the Mediterranean coastal towns [7], it undergoes rapid population growth and rapid expansion of urban areas in an undersigned manner mostly. The urban environment in Idku is characterized by high densities in the south adjacent to the road and moderate to low densities and mixed land-uses as approaching the Mediterranean coastal barren land/ bare soil. The town has been expanding rapidly during the last two decades. Such rapid expansion was largely motivated by transportation network development and population growth. The physical setting of the surrounding landscape is mostly barren land/bare soil (Figure 1).

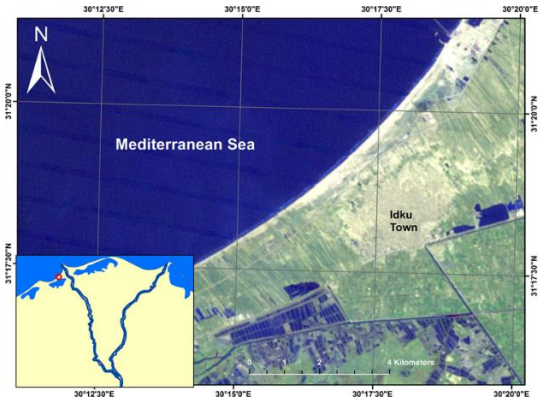

Figure 1. Situation of Idku Town

2.2 Data source

To detect changes in the urban areas in Idku, two multi-temporal Landsat images are used with a time span of 18 years (Table 1). The Idku Town is covered by the scenes of path 177 and row 38. Both scenes are cloud-free and high quality. No atmospheric correction has been performed for the data. Sub-scenes covering the Idku Town and its surroundings are clipped from the original scenes for data analysis.

Table 1. Landset scene metadata

Year	Satellite	Sensor	Path	Row	Date
1998	Landsat 5	TM	177	38	11-04-1998
2016	Landsat 8	OLI/TIRS	177	38	18-04-2016

2.3 Methodology

The developed methodology is based on separating urban areas from their surrounding barren land and bare soil through utilizing the thermal band. It is well-known that urban areas can cause land surface temperature (LST) to increase in a phenomenon known as "heat island" [2, 9]. Such urban heat island can be used to better separate built-up areas from other land covers [22] such as water and vegetation. But barren land and bare soil emit more energy in the thermal band compared to the built-up areas. Therefore, applying a careful threshold can separate both. The difference in emitted heat between both of them is not huge but it is sufficient to define a threshold.

The extraction process of the built-up areas can be performed according to the following steps which are illustrated in Figure 2:

Step 1: Generate the indices images

There are three general land covers in the sub-scene image which are vegetation, land and water. These land covers are enhanced using specified indices which depend mostly on the spectral properties of these land covers (Figure 3). Three indices were used to reduce the redundancy of multispectral data and maximize the difference among different land covers. These indices are: Soil-Adjusted Vegetation Index (SAVI), Normal Difference Built-up Index (NDBI) Modified Normal Difference Water Index (MNDWI). The multispectral bands of each image are used to generate the three indices: SAVI, NDBI and MNDWI using the equations given in Table 2. Therefore, each multispectral image would generate three images each of which represented one of the up mentioned indices. SAVI was used to discriminate vegetation from soil. It is considered to be a better replacement for the well-known Normal Difference Vegetation Index (NDVI) because it is more sensible for the low plant cover as in built up areas [17] and in low vegetated agricultural land. SAVI can discriminate vegetation in an area of plant cover as low as 15%, whereas NDVI can only discriminate vegetation effectively in an area when the plant cover is higher than 30% [25]. SAVI has more advantage of the remarkable reflection of vegetation in the near infrared (NIR) region of the spectrum when compared to the red one. In the used sub-scenes, the vegetation cover is moderate, therefore, a value of 0.5 was assigned to the "I" term in the SAVI equation. NDBI has the advantage of the unique response of the built-up areas in which they have higher response in the middle infrared (MIR) than in the NIR [20] to discriminate them from their surroundings. This would hold true in areas of healthy vegetation and water bodies. However, some vegetation under certain circumstances of dryness would have high values in MIR and sometimes even higher than in the NIR resulting in positive values under the NDBI [27, 28] and get confused for the urban areas. The same goes for barren land/bare soil and accordingly they are misclassified as built-up areas, which is the case in our case study. MNDWI developed by Xu [29], was employed to enhance the NDWI to better discriminate between water and built-up areas as both reflect green light more than reflect NIR light [17]. MNDWI used the MIR instead of the NIR in the NDWI (Table 2).

Step 2: Replace the multispectral image by the different indices' images

The multispectral data with their high redundancy is replaced by indices so that the differences among the major land covers are maximized.

Step 3: Apply principal component analysis (PCA) to the indices' images

Principal Component Analysis (PCA) is used to reduce the interference among different land covers produced by the three indices. The three indices' images represent the input for the PCA

to generate three principal components (PCs). The first principal component (PC1) contains most of the data (about 90% of the data) then followed by the second and third principal components (PC2 and PC3). The amount of data contained in each PC is given in Table 3.

Step 4: Choose the PC in which the land is most discriminated from other features

Out of the three PCs, there is one PC image in which the land features are more discriminated than both water and vegetation. This would appear in one of the PCs as areas of either remarkable brightness or darkness according to the sign of its value (if the sign is positive, land features would appear as bright areas while negative value means dark areas). The PC that reveals the land sharply either in positive or negative values (bright or dark features, respectively) was selected. Determining the suitable PC could be attained by analyzing the Eigen vectors and Eigen values for each date. In the chosen PC, land features would have an Eigen vector with a sign that is opposite to those of both water and vegetation.

Step 5: Separation of land

The chosen PC was then employed to extract the built-up areas in an automated manner by the means of applying a threshold [17]. By applying a careful threshold on the chosen PC image, the land areas which contain both built-up areas and barren land/bare soil, are separated from both water and vegetation. The resulting image would be a land-only image.

Step 6: Generate a mask image out of the land-only image

The land-only image was converted into a binary image in which all values of land are given as a value of 1 and elsewhere as a value of 0.

Step 7: Extract the thermal values corresponding to the land

The generated mask was multiplied by the thermal band of the original data (band 6 for 1998 image and band 10 for 2016 TIRS image) to generate an image which contains the thermal range of land. In the land-thermal-range image, the built-up areas would appear darker than the barren land/bare soil areas.

Step 8: Extract the built-up areas

By applying a careful threshold on the thermal values of land, land class is separated into two subclasses: built-up areas and barren land/bare soil areas. The difference between the thermal values of the built-up areas and the barre land/bare soil is not huge but it is enough to differentiate between them. The threshold choice in this step is crucial and requires a great deal of attention. The built-up areas are given a value of 1 and elsewhere in the image is given the value of 0. The resulting image represents the built-up areas with a minimal noise from barren land/bare soil.

Finally, the accuracy of the resulted thematic images was assessed using 256 randomly distributed points. The same exact points have been employed for both images. Visual interpretation has been applied to check on the points using False Color Composite (30 m) of RGB 7, 5, 2 for the L5, 1998 image and a High Pass Filter (HPF) panchromatic sharpened image (15 m) with RGB 7, 5, 2 for the L8, 2016 image.

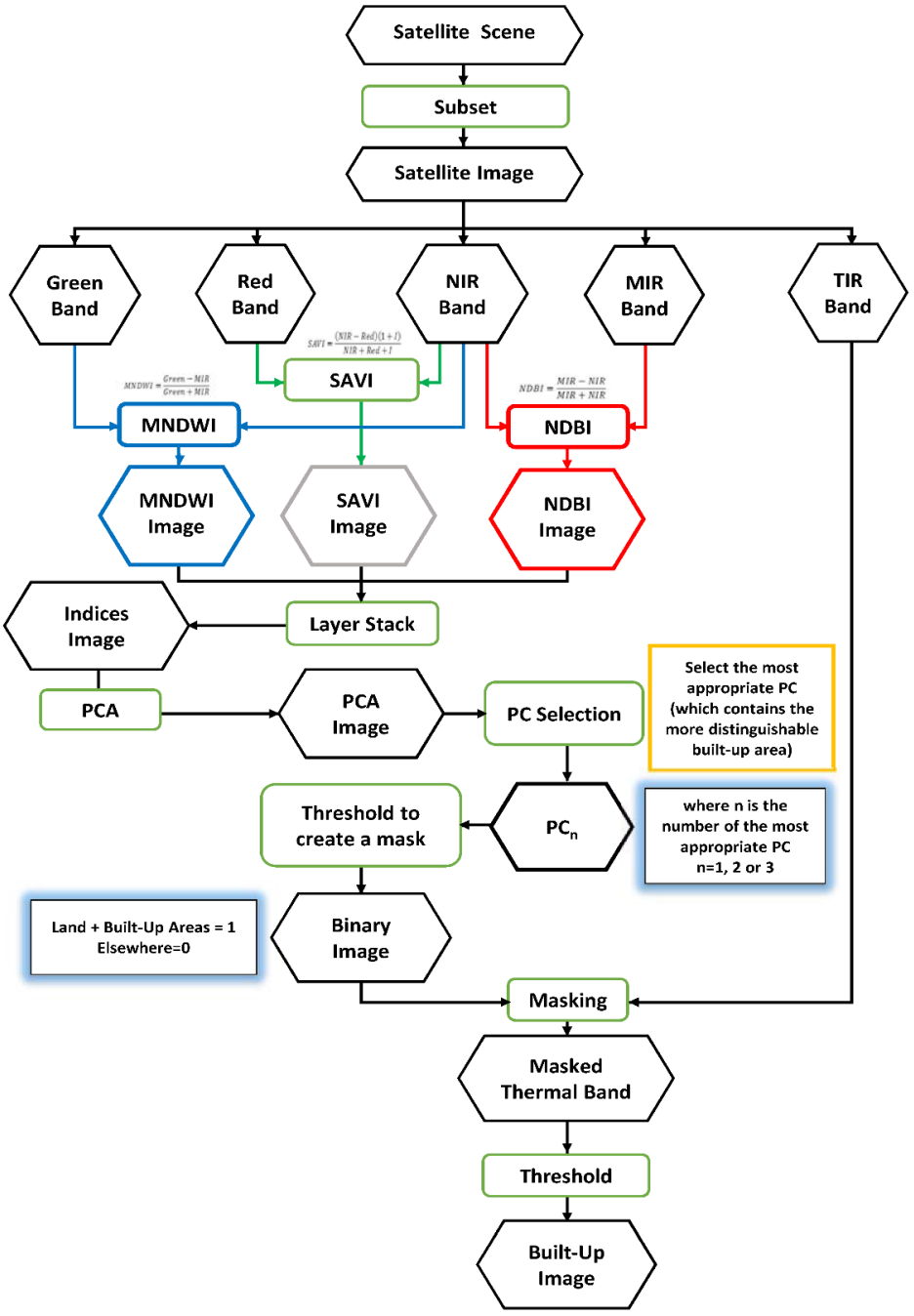

Figure 2. Methodology for semi-automated built-up area extraction

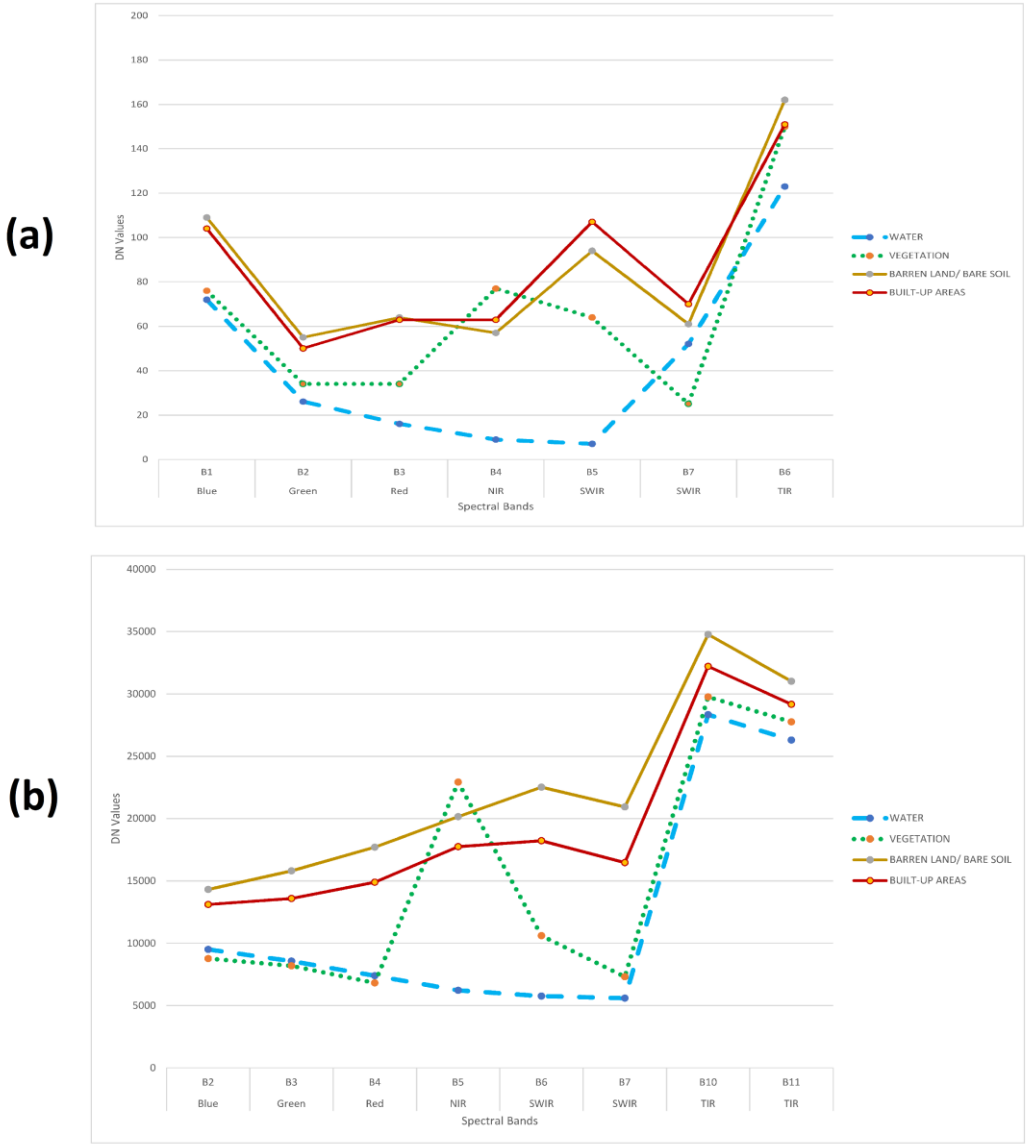

Figure 3. Spectral signatures of different land covers for (a) L5 TM image for the year 1998 and (b) L8 OLI/TIRS image for the year 2016

Table 2. Different indices and the formulae used to generate them

Indices	Formulae	Reference
SAVI	$SAVI = \frac{(NIR - Red)(1 + I)}{NIR + Red + I}$	[25]
	Where I is a correction factor that ranges from 0 (in case of dense vegetation cover) to 1 (in case of lack of vegetation or a very low vegetation cover).	
NDBI	$NDBI = \frac{MIR - NIR}{MIR + NIR}$	[20]
MNDWI	$MNDWI = \frac{Green - MIR}{Green + MIR}$	[27]

3. Results and Discussion

The three-indices images for the years 1998 and 2016 are illustrated in Figure 4 whereas Table 3 shows the Eigen vector and Eigen values of the principal component analysis of the multi-temporal indices. The second principle component (PC2) is the one in which built-up areas are most distinguished from water and vegetation as the different sign indicates. The positive sign of the NDBI Eigen vector indicates areas of brightness in the PC 2 whereas negative values of SAVI and MNDWI Eigen vectors indicate areas of darkness (Figure 5).

Table 3. Eigen vector and eigen values of the principal component analysis of the multi-temporal indices

	INDICES	1998			2016		
	IMAGES	*PC1*	*PC 2*	*PC 3*	*PC1*	*PC 2*	*PC 3*
	SAVI	0.74	-0.53	0.42	0.89	-0.18	0.43
Eigen Vectors	*NDBI*	0.07	0.68	0.73	-0.24	0.60	0.76
	MNDWI	-0.67	-0.51	0.54	-0.40	-0.77	0.49
% Eigen Values		90.9	8.8	0.3	92.9	6.9	0.2

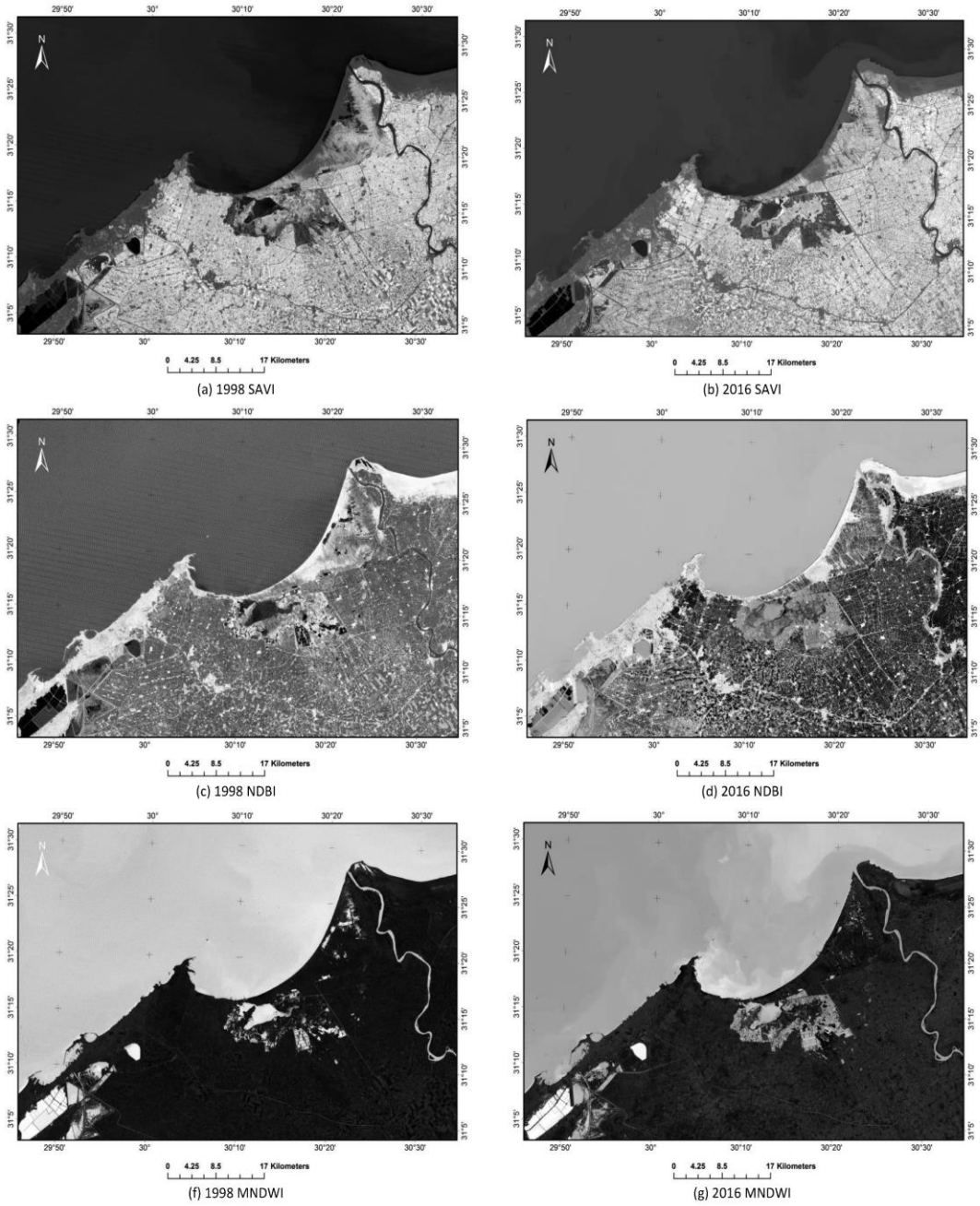

Figure 4. Indices images for multi-temporal sub-scenes

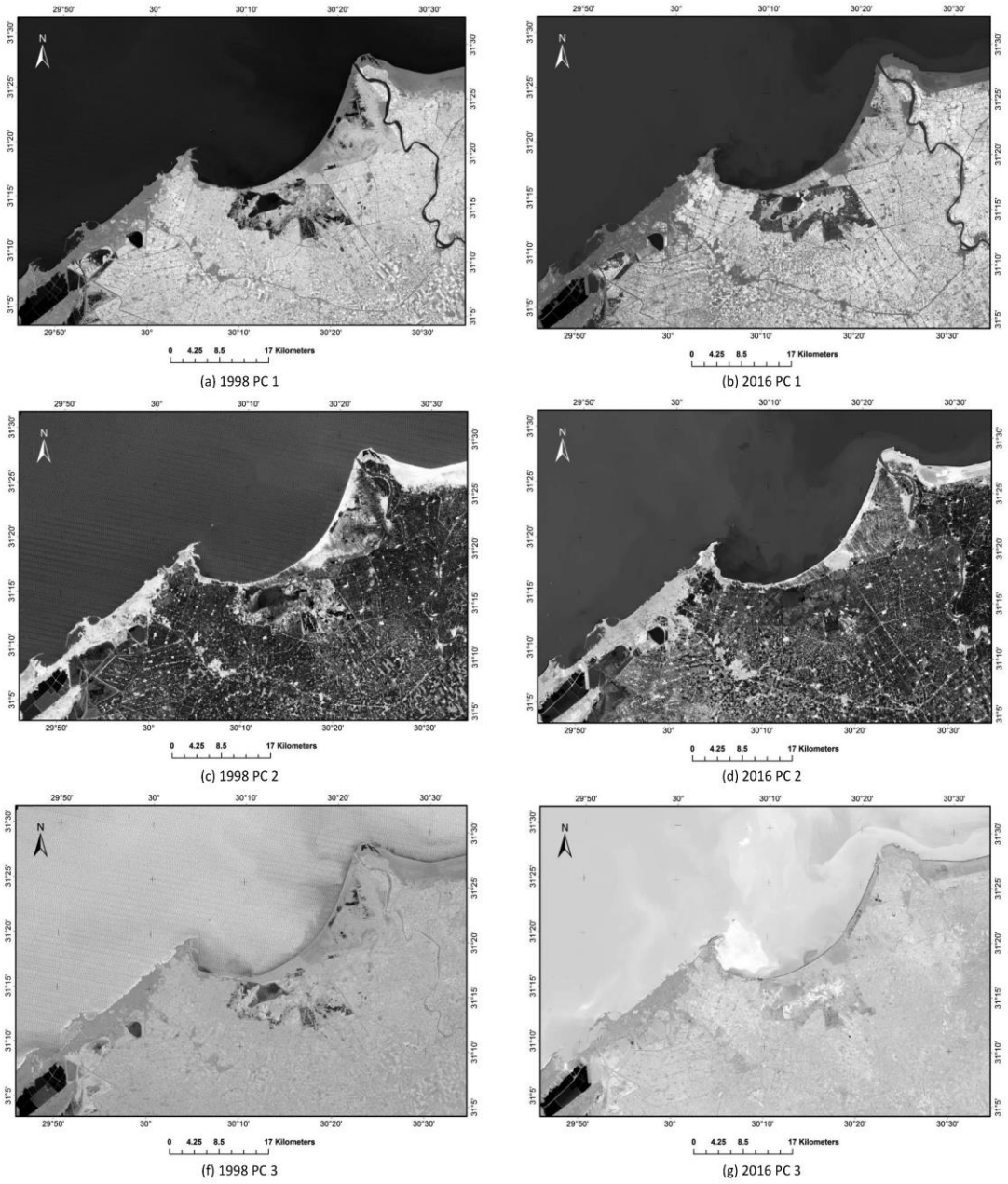

Figure 5. Principal component analysis (PCA) for the multi-temporal index images

Figure 6 shows the histograms of the second principal components (PC2s) of the indices' images for the years 1998 (a) and 2016 (b). The x-axis of the histogram represents the PC2 values while the y-axis refers to the frequency which means how many pixels are belonging to a certain value. The last peak of the histogram represents the values of the land as these values are the highest values of the image. The low frequency of the peak is due to the land that is not the dominating feature in the image. Applying a threshold to separate the values of the last peak would result in the separation of land values from the image. A threshold of 0.2 and a double threshold of 0.05 and 0.15 for the PC 2 of the 1998 and 2016 images, is applied to extract the land features as shown in Figure 6. Figure 7 shows the extracted land features for the multi-temporal sub-scenes. This method is successful in regard to extracting land features from water and vegetation. However, it can not differentiate between built-up areas and their adjoining barren land and bare soil. Therefore, the need for the thermal band integration arose.

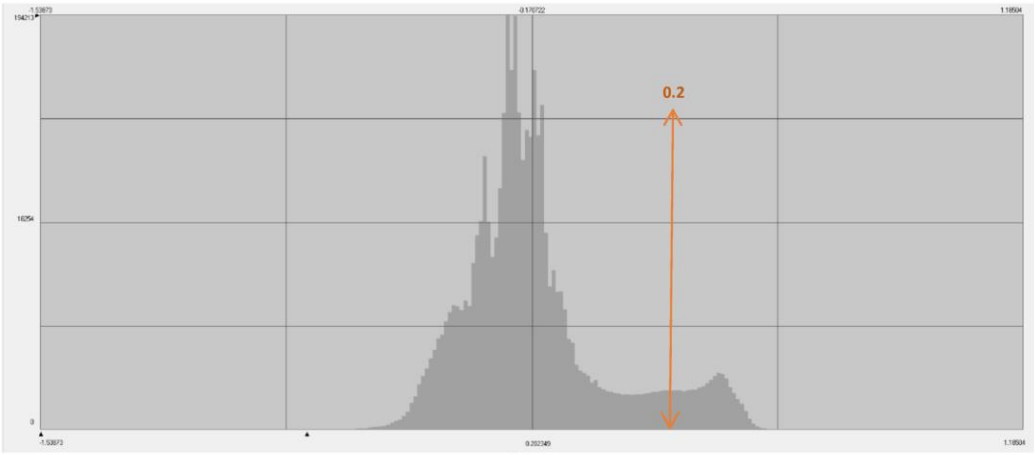

(a)

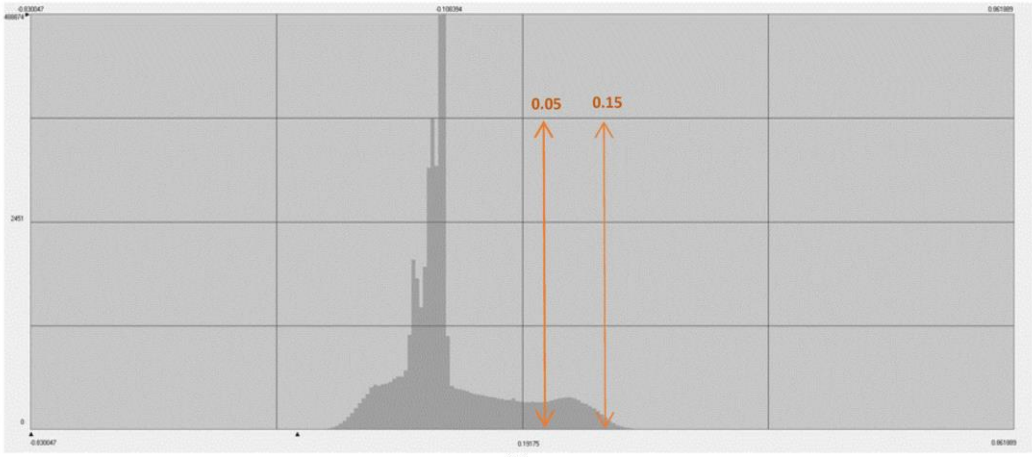

(b)

Figure 6. Histogram of the PC 2 with the threshold(s) for the years (a) 1998 and (b) 2016

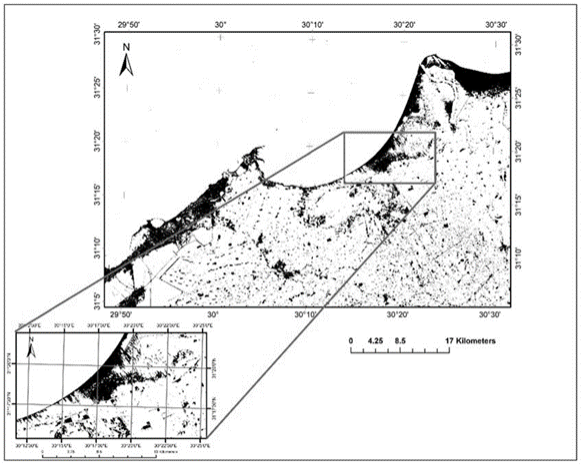

(a) 1998

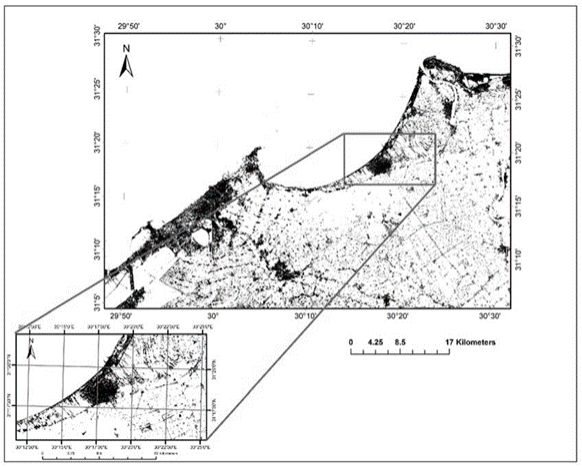

(b) 2016

Figure 7. Extracted land features from the multi-temporal indices PC2 images for the years (a) 1998 and (b) 2016 and the Town of Idku is zoomed-in

The thermal values for the land features were separated in a new image (land-only thermal image). Then a threshold was applied to separate built-up areas and barren land/ bare soil. A double threshold has been assigned to extract thermal ranges of 152 to 157 and 29400 to 33800 out of the land thermal values of the years 1998 and 2016, respectively. These ranges have been found to be corresponding to built-up areas. The built-up areas' separation is thus much enhanced and the borders of the town is much more realistic (Figure 8). The idea behind the thermal band integration in differentiating built-up areas from barren land/bare soil is that built-up areas are course textured-areas reflecting more light than the smooth-natured barren land/ bare soil does. As built-up areas reflect more light, they are expected to emit less light. This is always the case; good reflectors are bad emitters and vice versa [28]. Although the proposed methodology is able to improve the extraction of the built-up areas, it can not totally eliminate barren land/bare soil from the scene, none of the methodologies does [7, 15, 17, 22]. But this methodology reduced the interference significantly and increased the accuracy of extraction remarkably.

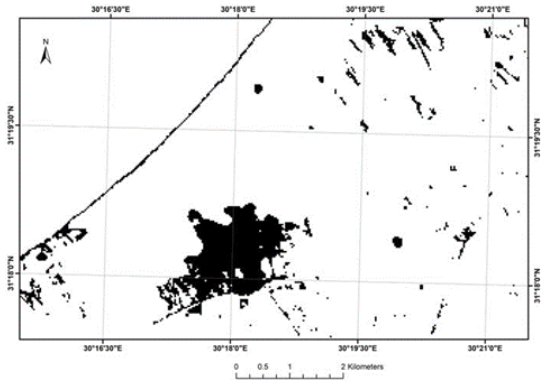

(a) 1998

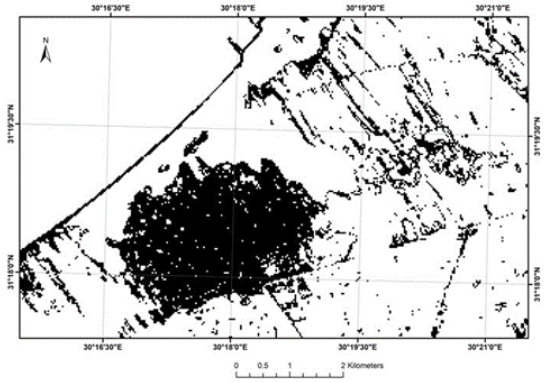

(b) 2016

Figure 8. Idku Town as extracted by integrating the thermal band for the years (a) 1998 and (b) 2016

The overall accuracies were found to be 96.48% and 93.39% with overall Kappa statistics of 0.6488 and 0.7305 for the images of the years 1998 and 2016, respectively (Table 4). For the image of L8, 2016, the panchromatic sharpened image allowed better error avoidance during the accuracy assessment due to the relative easiness of visual interpretation compared to the unsharpened RGB image. Unfortunately, this was not the case for the L5, 1998 image due to the absence of the panchromatic band.

The coarse resolution of the thermal band compared to other multispectral bands (60 m for ETM+ and 100 m for TIRS) does not much affect the accuracy of estimation in this study as it is concerned with the urban form expansion of Idku Town. Therefore, the border of the town is what matters. Mixed pixels of concern would be restricted only to those on the margin of the town. These mixed pixels could be a source of error together with the different resolution of both L5 and L8 thermal bands but compared to the bulk urban area of the town, it would be much like applying a

filter to smooth its appearance. In case of using the same sensor, the error would be distributed evenly through different scenes and the changes in urban areas would still hold true.

Spatial analysis of urban form extracted from remotely-sensed data showed that the built-up area of Idku Town has expanded from 2502 km^2 in 1998 to 8003 km^2 in 2016. This means that the built-up area has enlarged three times its original area in 1998 with an annual expansion rate of about 12% during almost 20 years. Such rapid expansion can be related mainly to demographic deriving forces as well as the construction of new road infrastructure. For instance, the population size of Idku Town increased from 87,848 in 1996 to 97,168 in 2006 [29, 30]. In addition, it was noted that the town expansion during this time span was directed towards the northern parts of the town. This is mainly due to two reasons, i.e. the construction of the International Coastal Highway in the north of the town in 2002 and the existence of Idku lake in the south of the town which acts as a natural barrier that hinders town expansion southward (Figure 9).

Table 4. Summary of accuracy assessment results

	1998					2016				
Class Name	Urban	Non-Urban	Total	Overall Accuracy	Kappa	Urban	Non-Urban	Total	Overall accuracy	Kappa
Urban	9	7	16	96.48%	0.6488	28	16	44	93.39%	0.7305
Non-Urban	2	238	240			1	212	213		
Total	11	245	256			29	228	257		

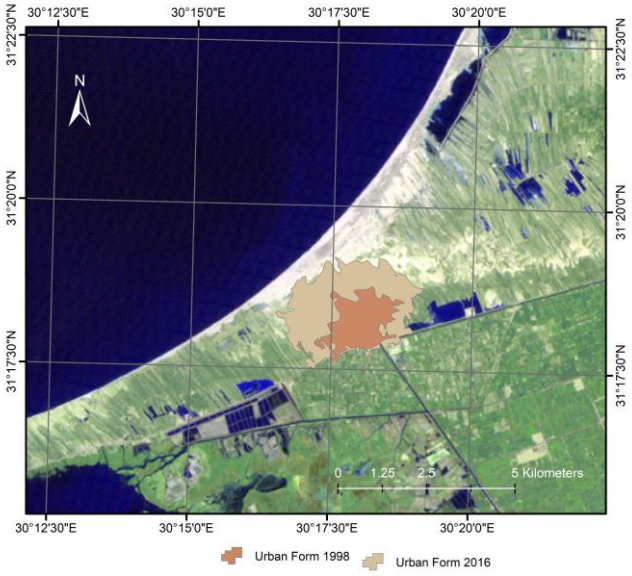

Figure 9. Urban Form Expansion from 1998 to 2016

4. Conclusions

It was revealed that the proposed methodology for delineating urban areas within barren land/ bare soil background in a semi-automated manner yielded satisfactory results. This developed methodology was capable of decreasing the high interference between the urban areas and their adjoining barren land/bare soil. The use of the thermal band to differentiate between these two classes was successful and increased the accuracy of the extraction in a remarkable manner. Furthermore, it was found that the coarse resolution of the thermal band compared to other multispectral bands (60 m for ETM+ and 100 m for TIRS) has marginal impact on the accuracy of estimation.

5. Acknowledgements

This research work is part of a research project sponsored by the IDRC-Canada for establishing Alexandria Research Center for Adaptation to Climate Change (ARCA) at Alexandria University, Egypt.

References

[1] Bernstein, J.D., 1994. Land use considerations in urban enviornmnetal management In: Urban management programme discussion paper, UMPP no. 12. Washigton D.C.: World Bank, pp. 9-26.

[2] Gartland, L., 2008. Heat islands: understanding and mitigating heat in urban areas [e-book] London: Earthscan. [online]. Available at: https://books.google.com.eg/books?id= wokqNDknbLIC>.

[3] Jusuf, S.K., Wong, N.H., Hagen, E., Anggoro, R., and Hong, Y., 2007. The influence of land use on the urban heat island in Singapore. *Habitat International*, 31(2), 232-242.

[4] Kim, H.H., 1992. Urban heat island. International Journal of Remote Sensing, 13(12), 2319-2336.

[5] Lo, C.P., 2004. Testing urban theories using remote sensing. GiScience & Remote Sensing, 41(2), 95-115.

[6] Oke, T.R., 1973. City size and the urban heat island. Atmospheric Environment (1967), 7(8), 769-779.

[7] Polydoros, A. and Cartalis, C., 2015. Use of earth observation based indices for the monitoring of built-up area features and dynamics in support of urban energy studies. *Energy and Buildings*, 98, 92-99.

[8] Weng, Q., Lu, D., and Schubring, J., 2004. Estimation of land surface temperature-vegetation abundance relationship for urban heat island studies. Remote Sensing of Environment, 89(4), 467-483.

[9] Yuan, F. and Bauer, M.E., 2007. Comparison of impervious surface area and normalized difference vegetation index as indicators of surface urban heat island effects in Landsat imagery. *Remote Sensing of Environment*, 106(3), 375-386.

[10] Zhao, S., Da, L., Tang, Z., Fang, H., Song, K., and Fang, J., 2006. Ecological consequences of rapid urban expansion: Shanghai, China. *Frontiers in Ecology and the Environment*, 4(7), 341-346.

[11] Fazal, S., 2000. Urban expansion and loss of agricultural land-a GIS based study of Saharanpur City, India. *Environment and Urbanization*, 12(2), 133-149.
[12] Villa, P., 2012. Mapping urban growth using soil and vegetation index and Landsat data: The Milan (Italy) city area case study. *Landscape and Urban Planning*, 107, 245-254.
[13] Weber, C. and Puissant, A., 2003. Urbanization pressure and modeling of urban growth: example of the Tunis Metropolitan Area. *Remote Sensing of Environment*, 86, 341-352.
[14] Waqar, M., Mirza, J., Mumtaz, R., and Hussain, E., 2012. *Development of new indices for extraction of built-up area and bare soil from landsat*. [Online] Available at: https://www.researchgate.net/publication/284816904.
[15] Xu, H., 2008. A new index for delineating built-up land features in satellite imagery. *International Journal of Remote Sensing*, 29, 4269-4276.
[16] Ma, Y. and Xu, R., 2010. Remote sensing monitoring and driving force analysis of urban expansion in Guangzhou City, China. *Habitat International*, 34, 228-235.
[17] Xu, H., 2007. Extraction of urban built-up land features from Landsat Imagery using a thematic oriented index combination technique. *Photogrammetric Engineering & Remote Sensing*, 73(12), 1381-1391.
[18] Cleve, C., Kelly, M., Kearns, F.R., and Moritz, M., 2008. Classification of the wildland-urban interface: A comparison of pixel- and object-based classifications using high-resolution aerial photography. *Computers, Environment and Urban Systems*, 32(4), 317-326.
[19] Guindon, B., Zhang, Y., and Dillabaugh, C., 2004. Landsat urban mapping based on a combined spectral–spatial methodology. *Remote Sensing of Environment*, 92(2), 218-232.
[20] Zha, Y., Gao, J., and Ni, S., 2003. Use of normalized difference built-up index in automatically mapping urban areas from TM imagery. *International Journal of Remote Sensing*, 24(3), 583-594.
[21] Zhang, Q., Pavlic, G., Chen, W., Fraser, R., Leblanc, S., and Cihlar, J., 2005. A semi-automatic segmentation procedure for feature extraction in remotely sensed imagery. *Computers & Geosciences*, 31(3), 289-296.
[22] Bhatti, S.S. and Tripathi, N.K., 2014. Built-up area extraction using Landsat 8 OLI imagery. *GIScience & Remote Sensing*, 51(4), 445-467.
[23] Xu, H., 2006. Modification of normalised difference water index (NDWI) to enhance open water features in remotely sensed imagery. *International Journal of Remote Sensing*, 27(14), 3025-3033.
[24] Sader, S.A., Hayes, D.J., Hepinstall, J.A., Coan, M., and Soza, C., 2001. Forest change monitoring of a remote biosphere reserve. *International Journal of Remote Sensing*, 22 (10), 1937-1950.
[25] Ray, T.W., 1994. *Vegetation in remote sensing FAQs*. [online]. Available at: http://www.remote-sensing.info/wp-content/uploads/2012/07/A_FAQ_on_Vegetation_in _Remote_Sensing.pdf.
[26] Varshney, A., 2013. Improved NDBI differencing algorithm for built-up regions change detection from remote-sensing data: an automated approach. *Remote Sensing Letters*, 4(5), 504-512.
[27] Xu, H., 2005. A study on information extraction of water body with the Modified Normalized Difference Water Index (MNDWI). *Journal of Remote Sensing*, 9(5), 511-517.
[28] Schowengerdt, R.A., 2007. *Remote Sensing: Models and Methods for Image Processing*. 3rd ed. USA: Elsevier Inc.
[29] CAPMAS, 1996. Population Census 1996 In. Cairo: Central Agency for Public Mobilization and Statistics, pp. 4.
[30] CAPMAS, 2006. Population Census 2006 In. Cairo: Central Agency for Public Mobilization and Statistics, pp. 4.